

Structure and dynamics of gold atomic chains grown on Cu(110): Experiment and theory

Georgios Kyriakou,¹ Federico J. Williams,¹ Mintcho S. Tikhov,¹ Adrian Wander,² and Richard M. Lambert^{1,*}

¹*Department of Chemistry, University of Cambridge, Lensfield Road, Cambridge CB2 1EW, United Kingdom*

²*CCLRC Daresbury Laboratory, Daresbury, Warrington WA4 4AD, United Kingdom*

(Received 6 July 2005; published 29 September 2005)

Gold deposition on Cu(110) results in nucleation and growth of periodic, triple-stranded chains of Au atoms parallel to $\langle 100 \rangle$. These structures have unusual properties that differ substantially for other nominally similar systems. The chains, initially zig-zag, nucleate and grow at the lowest coverages, exhibit lateral mobility, straighten up as coverage increases, are robust against intermixing with the substrate, and maintain registry across step edges. Molecular dynamics simulations and electronic structure calculations provide good insight into all these properties, including details of the growth mode. It appears that gold chain packing density is limited mainly by strain in the underlying copper, rather than chain-chain interactions.

DOI: [10.1103/PhysRevB.72.121408](https://doi.org/10.1103/PhysRevB.72.121408)

PACS number(s): 68.43.Hn, 68.43.Fg, 68.43.Bc, 68.37.Ef

Patterning of surfaces of all kinds on a truly nanometric scale continues to attract attention with respect to fundamental properties and in regard to potential applications in a variety of fields. A diverse range of top-down and bottom-up methodologies has been used including extreme ultra violet lithography,¹ dip-pen lithography,² and molecular manipulation with scanned probes.^{3,4} Deposition/self-organization provides a route for nanoscopic patterning of surfaces over large areas with both inorganic materials⁵ and organic molecules.⁶ Here we report unusual and interesting behavior exhibited by gold when deposited on the Cu(110) surface at room temperature. Under such conditions, on the (100) (Refs. 7 and 8) and (111) surfaces,⁹ intermixing and alloy formation occurs, which is consistent with the bulk miscibility of the metals which form stable alloy phases.¹⁰ In the present case however, chains of gold atoms are formed on an otherwise bare copper surface, their periodicity varying continuously with Au coverage. Moreover, the chain direction is not parallel to the $\langle 110 \rangle$ channels, but perpendicular to them. Modeling by means of calculations based on Sutton-Chen potentials provides an explanation for the lowest coverage structures in which the STM images reveal disordered, zig-zag chains. Full *ab initio* simulations of complete chains have also been performed to investigate their equilibrium electronic and geometric structure.

Experiments were carried out in an Omicron UHV STM instrument equipped for LEED and Auger spectroscopy. Images were acquired in constant current mode ($I_T=2.5$ nA) under both negative and positive bias; Au deposition was carried out by vacuum evaporation of gold from a collimated, resistively-heated source at a rate of 0.1 ML/min with the Cu sample held at room temperature; all subsequent measurements were made at room temperature. Gold coverages are specified in monolayers (ML) and are estimated directly from the STM images—they are in reasonable quantitative agreement with corresponding values estimated by Auger spectroscopy (within $\sim 25\%$). In order to gain insight into the atomic structure and dynamical behavior of the Au chains, we performed simulations using Sutton-Chen potentials¹¹ within the GULP code¹² and *ab initio* plane wave density functional calculations using the CASTEP code.¹³

Figure 1 shows a $1000 \text{ \AA} \times 1000 \text{ \AA}$ STM image of periodically distributed gold chains resulting from room temperature deposition of ~ 0.2 ML Au on an initially clean Cu(110) surface. Interestingly, the $\langle 001 \rangle$ -oriented chains maintained registry across the step edges that run along the $\langle 110 \rangle$ direction. Their average spacing was $\sim 30 \text{ \AA}$ with apparent widths of $3\text{--}6 \text{ \AA}$, which corresponds to single or double stranded chains of gold atoms—a point we return to below. Figures 2(a)–2(d) are $500 \text{ \AA} \times 500 \text{ \AA}$ images that depict the evolution of surface structure with increasing Au loading. It is noteworthy that the chains nucleated and grew from the very lowest coverages (~ 0.1 ML), their spacing decreasing continuously with increasing Au coverage [e.g., Figs. 1(a) and 1(c)]; note also that the degree of “dither” decreases with increasing chain density and that the tendency for registry to be maintained across step edges persists even at the lowest coverage [Fig. 2(a)].

Two consecutive STM images taken at ~ 0.1 ML Au are shown in Figs. 3(a) and 3(b): it is clear that these images are nonidentical, suggesting that the gold structure is mobile along $\langle 110 \rangle$ room temperature: this would also account for the variability in apparent chain width observed at higher coverages. The STM and Auger data are in good accord with LEED observations. Thus the ~ 0.1 , ~ 0.13 , and ~ 0.2 ML structures [Figs. 2(a)–2(c)] characterized by ~ 50 , ~ 40 ,



FIG. 1. (Color online) STM image of Cu(110) after deposition of ~ 0.2 ML of Au ($1000 \times 1000 \text{ \AA}^2$, $I=2.5$ nA, $V_{\text{tip}}=-1$ V).

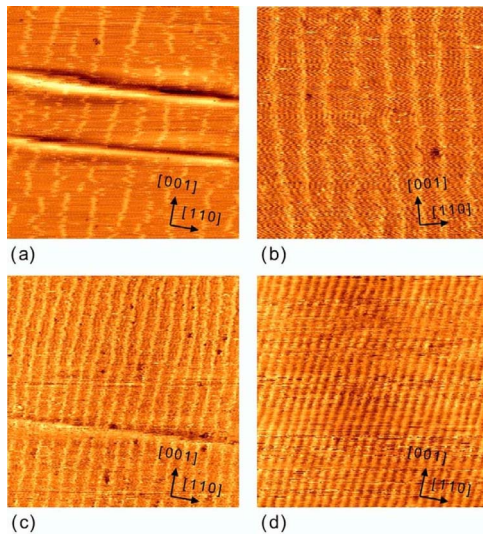


FIG. 2. (Color online) STM images showing evolution of surface structure with increasing Au coverage. (a) 0.1 ML Au; (b) 0.13 ML Au; (c) 0.2 ML Au; (d) 0.4 ML Au ($500 \times 500 \text{ \AA}^2$, $V_{\text{tip}} = -1 \text{ V}$, $I = 2.5 \text{ nA}$).

$\sim 30 \text{ \AA}$ interchain spacing, all gave 1×1 LEED patterns. A weak $p(9 \times 1)$ LEED pattern was observed at $\sim 0.25 \text{ ML}$; this evolved through a $p(8 \times 1)$ structure to yield a $p(7 \times 1)$ structure as the coverage increased to 0.4 ML. This final phase corresponds to unit cell dimensions of $17.9 \text{ \AA} \times 3.6 \text{ \AA}$ along $\langle 110 \rangle$ and $\langle 001 \rangle$, respectively, which matches very well the average chain separation measured by STM ($\sim 18 \text{ \AA}$).

The formation at room temperature of chain structures along the $\langle 001 \rangle$ direction of other (110) metal surfaces has been previously reported for Au on Ni (Refs. 14 and 15) and Ag on Cu (Ref. 16) at room temperature. However, our observations stand in marked contrast to these earlier cases in both of which extensive intermixing of the two metals occurred in the 0–0.4 ML coverage regime, chain structures appearing only above the 0.4 ML threshold. Accordingly, we carried out (i) simulations using Sutton-Chen potentials^{11,12} and (ii) *ab initio* plane wave density functional calculations¹³ in order to gain insight into the nature of our system.

Static geometry optimizations were performed for chains comprising 3–6 strands of Au atoms using a 7×1 unit cell. The stable structures were found to be chains containing either three or six strands of Au, both of which adopt a pris-

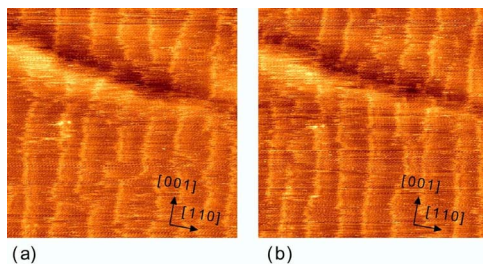


FIG. 3. (Color online) Consecutive scans of the same area taken after deposition of $\sim 0.1 \text{ ML}$ of Au on Cu(110) at room temperature ($500 \times 500 \text{ \AA}^2$, $V_{\text{tip}} = -1 \text{ V}$, $I = 2.5 \text{ nA}$).

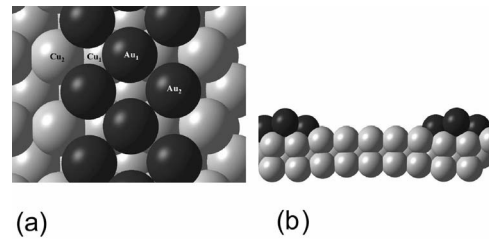


FIG. 4. (a) Plan view and (b) side view of the fully relaxed *ab initio* structure. The structure derived from the use of Sutton-Chen potentials is qualitatively similar.

matic structure. The lower Au atoms sit off-center in fourfold hollow sites on the Cu(110) surface with the second layer atom(s) sitting in the fourfold hollow site formed by the first layer. Only the 3-strand chain is consistent with the STM images and is illustrated in Fig. 4. This structure was therefore used as the basis for subsequent simulations, as follows. A single 3-strand Au chain was placed in a 14×4 Cu unit cell; 4 isolated adatoms were added to this system and molecular dynamics simulations were then performed for $T = 300 \text{ K}$. Interestingly, the Au adatoms were relatively immobile, whereas the gold chain was very mobile parallel to the $\langle 110 \rangle$ channels of the Cu surface—in excellent accord with experiment. As the chain moved about the surface it swept up the isolated Au adatoms. Simulations run at 1000 K showed different behavior. In this case the Au adatoms became unstable with respect to diffusion into the bulk. Additionally, the bottom layer atoms in the Au chains tended to displace Cu atoms from the first layer of the copper substrate, these then decorating the edges of the Au chain. This would appear to signal the onset of intermixing and alloy formation, although the simulations could not be run for sufficient time to follow this process in detail. These findings provide important confirmation of our interpretation of the STM images as being due to pure Au chains on a pure Cu substrate—unlike Cu(111)/Au (Ref. 9) and Cu(100)/Au (Refs. 7 and 8) where room temperature intermixing of the two metals occurs readily. They also point up the marked difference between the present case and Au/Ni(110) (Refs. 14 and 15) and Ag/Cu(110) (Ref. 16), where an initial intermixing stage is followed by chain growth only when the coverage exceed 0.4 ML; here the simulations demonstrate that isolated chains are stable—mimicking the experimental observation that chains nucleate and grow even at the lowest coverages attainable.

Static simulations were also run within 7×4 and 7×7 unit cells in order to mimic the process of chain growth in the high coverage regime. First, the 7×1 structure was constructed with complete 3-strand chains. Supercells of this system along the $\langle 001 \rangle$ chain direction were then set up, removing Au atoms so as to create gaps in the chains. Au adatoms were then added at all high symmetry adsorption sites. For the 7×4 unit cell a four atom gap is possible, whereas for the 7×7 cell larger gaps are possible, as shown in Fig. 5. These simulations reveal that growth does not proceed via attachment of additional Au atoms to the end of the 3-strand structure. Instead, Au atoms attached to the side of the chain end at sites 1 and 2 shown in Fig. 5(a), forming an

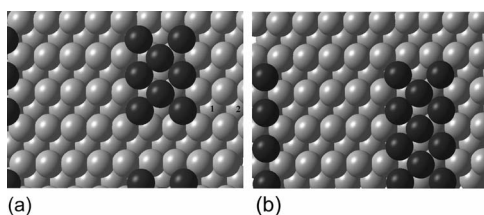


FIG. 5. Unit cells used to simulate chain growth; (a) 7×4 unit cell with a four atom gap (b) a 7×7 unit cell with a 7 atom gap. During chain growth the first adatom joins the chain at site 1 and the second at site 2. Only when three atoms are added do they attach to the end of the chain.

L-shaped object. Only with the addition of a *third* adatom did the end of the chain become the stable point of attachment. This accounts for the low coverage STM images [Figs. 2(a) and 2(b)] in which the chains have a disordered, zig-zag form. The zig-zag character is due to atoms being added to the sides rather than the ends of incomplete chains. Only when the coverage becomes sufficient to complete the chains do they straighten.

Attempts were made to simulate the chain formation process by using randomly distributed Au atoms as the starting point for molecular dynamics simulations. These rapidly aggregated to form amorphous clumps, elongated in the $\langle 001 \rangle$ direction, roughly in agreement with observation. However, our chain growth simulations show that the elongation step requires simultaneous attachment of *three* Au atoms to the end of the nucleated chain: this is likely to be a rare event, inaccessible on the time scale of our calculations.

Finally, the three-strand chain was used as a starting geometry for a full structural optimization using *ab initio* plane wave density functional theory. The calculation was performed within the 7×1 unit cell using the CASTEP code¹³ and the equilibrium structure results are illustrated in Fig. 4(b). The two center Cu atoms are depressed by 0.455 \AA and move towards each other by 0.13 \AA ; this buckling extends into the bulk to a depth of at least three layers. Details are given in Fig. 4(b) and Table I. Figure 4(b) reveals that the presence of the Au chains leads to a significant distortion of the Cu surface and gives rise to a “bowing” of the surface

TABLE I. Details of the optimized *ab initio* structure. The subscripts are labels defined in Fig. 4(a).

Bond length	Value (\AA)
Au ₁ —Au ₁	3.60
Au ₁ —Au ₂	2.89
Au ₁ —Cu ₁	2.60
Au ₂ —Cu ₂	2.68
Cu ₁ —Cu ₁	2.45
Cu ₁ —Cu ₂	2.57
Vertical spacings	
Cu ₁ —Cu ₂	0.455
Cu ₂ —Au ₁	1.171
Au ₁ —Au ₂	0.665

layers. This relatively deep distortion of the underlying Cu by the Au chain could transmit across monatomic step edges, thus accounting for the experimentally observed maintenance of chain registry across steps. In addition, the distortion of the Cu lattice will give rise to significant stress within the surface Cu layer. As the packing of the Au chains is increased, this stress must also increase. It is likely that the $7 \times$ periodicity reached at the maximum coverage is limited by the build up of this surface stress rather than by any long range interactions between the adsorbed Au chains. The *ab initio* structure is qualitatively similar to the Sutton-Chen structure. The principal difference is that the Sutton-Chen model produces a smaller buckling of the first copper layer (0.29 \AA compared to 0.455 \AA from the *ab initio* theory) and consequently the Au chain is less compact (extends further into the vacuum) within the pair potential model.

In summary, experiment and theory show that the Cu(110)/Au system possesses unusual characteristics that differ substantially from apparently closely related systems. Molecular dynamics simulations and electronic structure calculations provide a satisfactory explanation of the principal features, including stability against alloy formation, lateral mobility of the Au chains, their mode of growth and the transmission of chain registry across step edges.

*Author to whom all correspondence should be addressed. Tel: +44 1223 336467; Fax: +44 1223 336362; email address: rml1@cam.ac.uk

¹H. H. Solak, D. He, W. Li, and F. Cerrina, *J. Vac. Sci. Technol. B* **17**, 3052 (1999).

²R. D. Piner, J. Zhu, F. Xu, S. H. Hong, and C. A. Mirkin, *Science* **283**, 661 (1999).

³M. F. Crommie, C. P. Lutz, and D. M. Eigler, *Science* **262**, 218 (1993).

⁴D. M. Eigler and E. K. Schweizer, *Nature (London)* **344**, 524 (1990).

⁵L. Yan, M. Przybylski, Y. Lu, W. H. Wang, J. Barthel, and J. Kirschner, *Appl. Phys. Lett.* **86**, 102503 (2005).

⁶S. Lukas, G. Witte, and Ch. Wöll, *Phys. Rev. Lett.* **88**, 028301 (2002).

⁷P. W. Palmberg and T. N. Rhodin, *J. Chem. Phys.* **49**, 134 (1968).

⁸D. D. Chambliss, R. J. Wilson, and S. Chiang, *J. Vac. Sci. Technol. A* **10**, 1993 (1992).

⁹C. Q. Noakes and P. Bailey, *Thin Solid Films* **394**, 15 (2001).

¹⁰M. Hansen, *Constitution of Binary Alloys*, 2nd ed., Metallurgy and Metallurgical Engineering Series (McGraw-Hill, New York, 1958).

¹¹J. L. Rodriguez-Lopez, J. M. Montejano-Carrizales, and M. Jose-Yacamán, *Appl. Surf. Sci.* **219**, 56 (2003).

¹²J. D. Gale, *J. Chem. Soc., Faraday Trans.* **93**, 629 (1997).

¹³M. D. Segall, P. J. D. Lindan, M. J. Probert, C. J. Pickard, P. J.

- Hasnip, S. J. Clark, and M. C. Payne, *J. Phys.: Condens. Matter* **14**, 2717 (2002).
- ¹⁴L. P. Nielsen, F. Besenbacher, I. Stensgaard, E. Lægsgaard, C. Engdahl, P. Stoltze, K. W. Jacobsen, and J. K. Nørskov, *Phys. Rev. Lett.* **71**, 754 (1993).
- ¹⁵L. P. Nielsen, F. Besenbacher, I. Stensgaard, E. Lægsgaard, C. Engdahl, P. Stoltze, and J. K. Nørskov, *Phys. Rev. Lett.* **74**, 1159 (1995).
- ¹⁶D. A. Hite, O. Kizilkaya, P. T. Sprunger, E. Lægsgaard, and F. Besenbacher, *Phys. Rev. B* **65**, 113411 (2002).